Laboratori Nazionali di Frascati

LNF-71/85

A. Cattoni, M. Piccolo and F. Ronga : A HIGH SENSITIVITY METHOD FOR MEASURING MAGNETIC FIELD INTEGRALS

Estratto da : Nuclear Instr. and Meth. 96, 573 (1971)

NUCLEAR INSTRUMENTS AND METHODS 96 (1971) 573–580; © NORTH-HOLLAND PUBLISHING CO.

A HIGH SENSITIVITY METHOD FOR MEASURING MAGNETIC FIELD INTEGRALS

A. CATTONI, M. PICCOLO and F. RONGA

Laboratori Nazionali del CNEN, Frascati, Italy

Received 10 May 1971

A prototype for measuring the field integral along the straight section occupied by the magnetic detector to be used at the storage ring Adone has been constructed. This instrument, made by an electromagnetic balance, has a sensitivity better than 2 G m.

1. Introduction

One of the problems to be solved in the construction of a magnetic detector to be used at the storage ring Adone, is the interference of this detector with the magnets of the storage ring[1]).

It is therefore necessary to have a means of measuring the field integral $\int B\mathrm{d}s$ along the straight section occupied by the magnetic detector and nulling this field integral with compensator magnets.

An idea of the behaviour of the detector field, as seen by the stored beams, is given in fig. 1.

The field in the segments A_1, A_2, A_3 is produced by the main coil, while the one at B_1 and B_2 is due to compensator magnets.

In order to avoid perturbations to the equilibrium orbit the following condition must be satisfied[2]):

$$\int B\,\mathrm{d}s \leqslant 2.5\ \mathrm{G\ m} \quad \text{(at injection)},$$

since the maximum available field for the main coil is 4.5 kG, the sensitivity of the magnetic field integral measurement must be at least 5×10^{-4}.

Any conventional field integral measurement using a (fixed) coil would not be feasible because of the size of the system and because it would not be possible in the available space to ensure mechanical stability of the coil within the limits of the needed sensitivity.

For this reason we have decided to use an electromagnetic balance consisting of a current carrying wire sensitized by two piezoelectric crystals.

2. Experimental set up

The method has been tested by a prototype consisting essentially of a copper wire, 5 mm in diameter stretched along the internal axis and fixed at either end of a tube, with a rectangular cross section, 2.5 m in length. Tube and wire are supported at the ends by two quartz crystals (see fig. 2), which measure the force component in the x-axis direction.

Four bronze-phosphorous strips, fixing the tube to a U support, prevent it from moving in the y-axis direction.

TABLE 1

Characteristics of piezoelectric crystals.

Quartz force transducers Kistler 9201	
Max measuring range	±50 kp
Resolution	0.1 gp
Sensitivity	480 pC/kp
Deformation at max load	12 μm
Linearity	±0.3%
Insulation resistance	$10^{14}\ \Omega$
Capacitance	22 pF

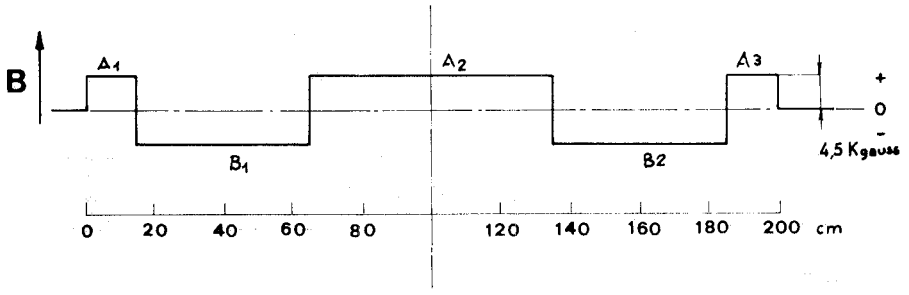

Fig. 1. Field in the radial plane of Adone magnetic analyzer.

A block scheme of the instrument is shown in fig. 3.

A low frequency oscillator (0.5–1.5 Hz) drives a power amplifier at the output of which there is a transformer with turns ratio 25:1 and band pass 0.3–10 Hz; the resulting low frequency current flowing in the wire is about 70 A. If the wire lies in a magnetic field directed along the y direction, there is a force acting on the wire which varies sinusoidally in the x direction and, in the very low frequency limit, is proportional to the integral of By along the wire.

The characteristics of piezoelectric crystals are listed in table 1.

In our series of tests the force on the wire when a 1 G magnetic field is applied was 1.7 g considerably more than the crystal's resolution, which is 0.1 g.

The crystal's outputs are connected to charge amplifiers (using MOSFET, Phylips type TAA 320) having input impedances $10^{11}\,\Omega$. The SF circuit indicated in fig. 3 sums output signals and provides suitable filtering through two double T serial filters. The band width of a typical filter we have used is shown in fig. 4.

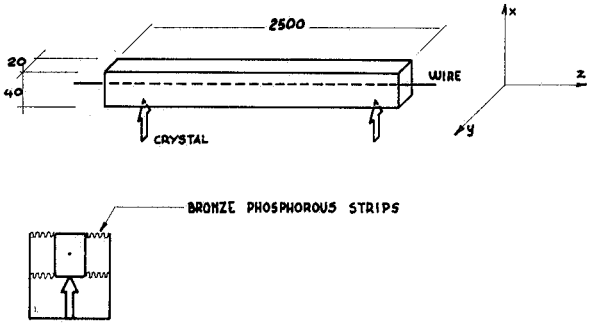

Fig. 2. Magnetometer scheme.

It is necessary to use filters owing to the background of the crystals output signals resulting from floor vibration and acoustical pickup. Furthermore, as we will discuss later, the filters are needed to reject signals two, three, four times the excitation frequency which are produced by magnetic field gradients. In designing filters care must be taken to obtain a narrow band pass as well as a fast rise time. The filter shown in fig. 4 has a rise time of 2–3 sec. The sum circuit output is fed into a classical sample-and-hold circuit in order to have a dc level at the output of the instrument. This sample-and-hold circuit is driven by another one which consists of a phase shifter, a discriminator and a monostable, in order to sample the input peak signal.

3. Magnetometer's response

The response of any dynamical system, subject to time dependent forces, in the absence of dumping, has poles at the resonating frequencies.

The time dependent forces applied to a system are transmitted without any dynamical contribution, only if the driving frequency is much less than the first resonance of the dynamical system.

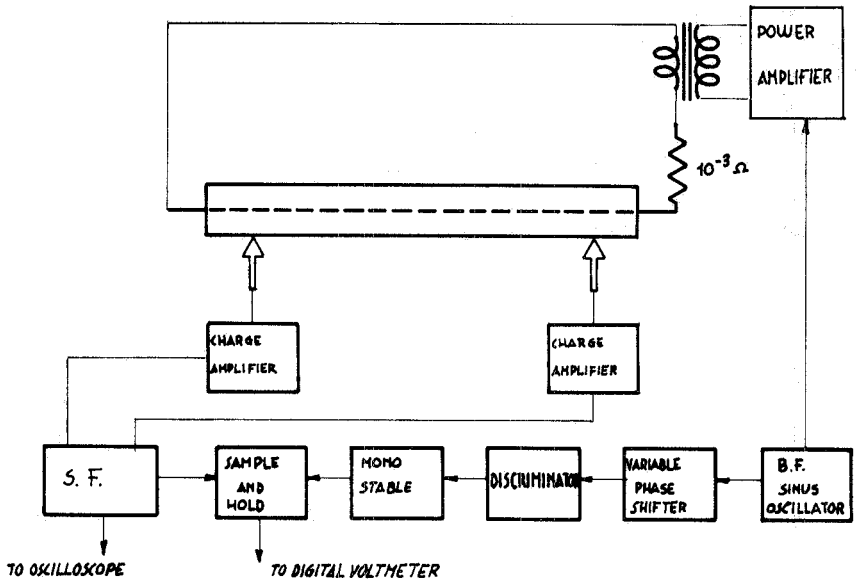

Fig. 3. Block diagram.

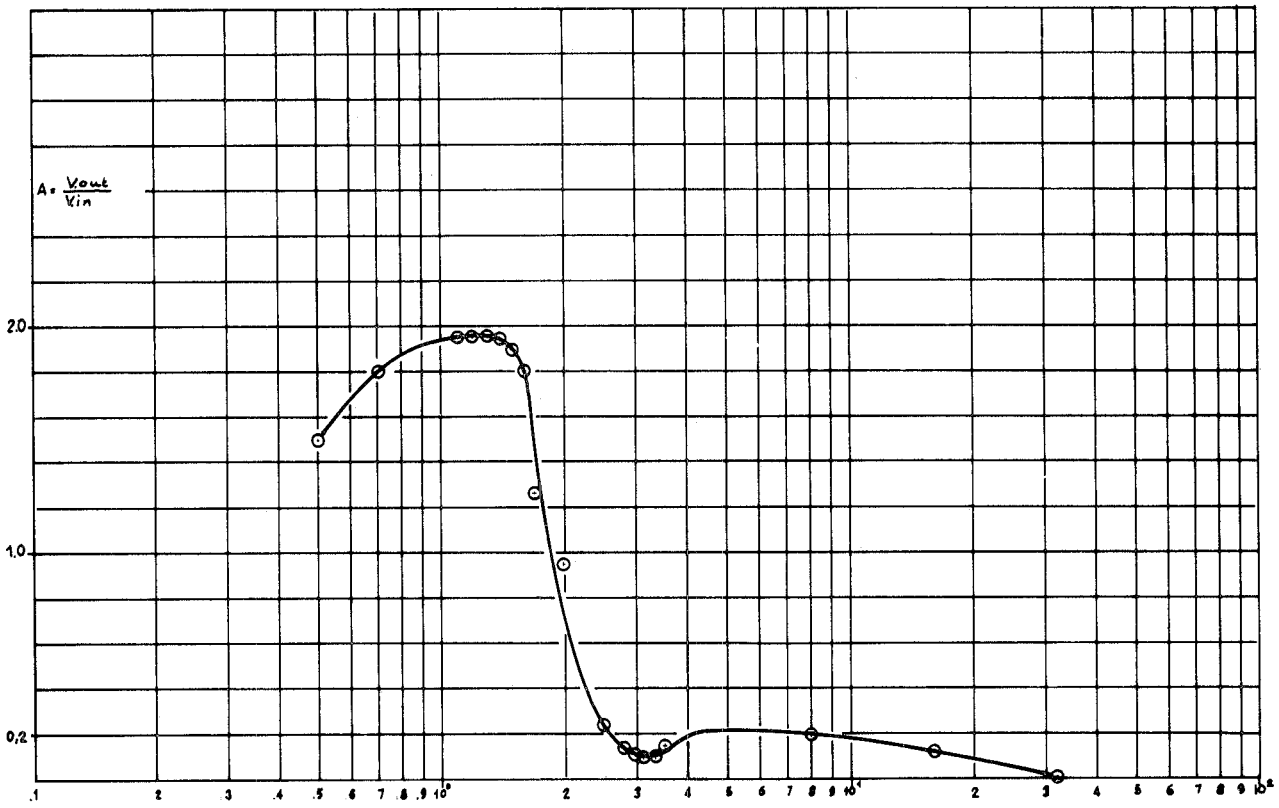

Fig. 4. Frequency response of a typical filter.

Our instrument described in the previous paragraphs consists of three oscillating systems:

a. clamped field sensing wire;
b. sustaining tube;
c. U-support.

TABLE 2

Resonance frequencies corresponding to two distinct values of the wire mechanical tension.

82 kg	140 kg	ν_{140}/ν_{82}
15.5	20	1.29
31.5	39	1.27
48	60	1.25
61	63	1.06
67	84	1.25
115	115	1.00

In table 2 resonance frequencies are listed corresponding to two distinct values of the wire mechanical tension.

There are two frequencies that are independent of the wire's tension and therefore are due to the mechanical structure of the support.

The table shows also that the dynamical response of the system, within the range 0–60 Hz is completely determined by the wire; hence we can schematically represent the magnetometer just as a vibrating string. The equation which describes a string of length L, subject to a force $f(x, t)$ per unity length, normal to its axis, is

$$T\frac{\partial^2 \eta}{\partial x^2} + f(x, t) = \mu \frac{\partial^2 \eta}{\partial t^2}, \tag{1}$$

where T is the mechanical tension, η is the wire displacement and μ is the wire linear density.

If we put

$$f(x, t) = F(x)\, e^{i\omega t}$$

and

$$\eta(x, t) = a(x)\, e^{i\omega t},$$

we obtain from (1)

$$\frac{d^2a}{dx^2} = -g^2a - \frac{F(x)}{T}, \tag{2}$$

where

$$g = \frac{\pi v}{Lv_0}, \quad v_0 = \frac{1}{2L}\left(\frac{T}{\mu}\right)^{\frac{1}{2}}, \quad v = \frac{\omega}{2\pi}.$$

For a given force distribution $F(x)$ the resultant constraint forces, R is

$$R = T\left[\frac{da}{dx}\bigg|_{x=L} - \frac{da}{dx}\bigg|_{x=0}\right]. \tag{3}$$

In the case of step distribution of forces:

$$F(x) = 0, \quad 0 < x < x_1,$$
$$F(x) = F, \quad x_1 < x < x_2,$$
$$F(x) = 0, \quad x_2 < x < L,$$

we obtain

$$R = \frac{F}{g}\left[-(\sin gx_2 - \sin gx_1) - (\cos gx_1 - \cos gx_2)\frac{1-\cos gL}{\sin gL}\right], \tag{4}$$

$$R \underset{gL\to 0}{\simeq} F\left[-(x_2-x_1)+(gL)^2 L\left(\frac{x_2^3-x_1^3}{6L^3} - \frac{x_2^2-x_1^2}{4L^2}\right)\right]. \tag{5}$$

Eq. (5) shows that the resultant constraint forces are equal to the integral of $F(x)$ (which corresponds to a static term) plus a dynamical term proportional to the square of the excitation frequency.

The linearity of eq. (1) allows the superposition principle to be applied to any arbitrary force distribution. For instance in the case of fig. 5 if we apply eq. (5) to each step and sum the results we get (since the integral of B is zero)

$$R = -iB(gL)^2(L/32), \tag{6}$$

where B is the magnetic field applied and i is the current flowing in the wire. If we want

$$\frac{R}{iB(L/2)} \leqslant 5\times 10^{-4},$$

we obtain, if $L = 2.5$ m,

$$v \leqslant v_0/35. \tag{7}$$

If there is damping with viscosity constant per unity length ξ, we have to substitute in eq. (5) for g^2

$$g'^2 = g^2 - j(\omega\xi/T). \tag{8}$$

In our case the dumping constant of the wire when no magnetic field is present, is

$$\xi = 10^{-2}\ \text{N sec/m}^2, \tag{9}$$

that is at very low frequencies, the correction is mall and the time constant of the dumping is about 25 sec.

When there is a magnetic field, there is a force per unity length due to induced currents given by

$$F'(x) = -j\frac{\omega B(x)}{Z}\int_0^L a(x)\,B(x)\,dx, \tag{10}$$

where $Z = R + j\omega L$ is the impedance of the circuit closed by the wire and $a(x)$ is the wire displacement.

Since in our case ($\omega = 3.14\ \text{sec}^{-1}$) Z is a pure resistance, $F'(x)$ is 90° out of phase with the excitation and therefore does not affect the measurement.

The damping effect of $F'(x)$ is quite strong: experimentally we have proved that in our conditions (see next section for details of the applied field) when the integral is zero the time constant for free oscillation damping is 2 sec.

Owing to dynamical displacement the wire grows longer with a subsequent tension change: eq. (1) can

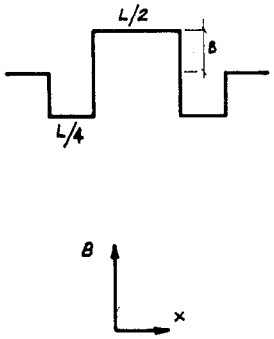

Fig. 5. Zero integral field distribution example.

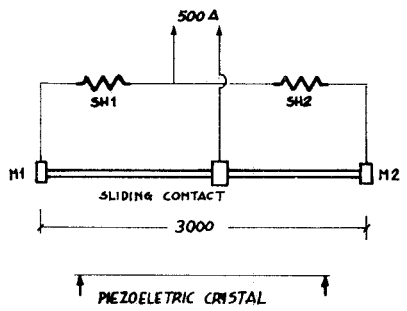

Fig. 6. Scheme of calibration disposal.

be modified to take into account tension terms resulting from dynamical displacement in the wire:

$$\left[T+\frac{ES}{2L}\int_0^L\left(\frac{\partial\eta}{\partial x}\right)^2 dx\right]\frac{\partial^2\eta}{\partial x^2}+f(x,t)=\mu\frac{\partial^2\eta}{\partial t^2}. \quad (11)$$

We can solve (11) with perturbative methods setting

$$\eta(x,t)=\eta_0(x,t)+\beta(x,t), \quad (12)$$

where $\eta_0(x,t)$ is the solution of (1), $\beta(x,t)$ is the correction. It can be shown that the resultant of the constraint forces is independent of $\beta(x,t)$.

If magnetic gradients are present in the region spanned by the wire one must also take into account the presence of corrective terms:

$$f(x,t)=B(x,0)\,i(t)+\left.\frac{\partial B}{\partial a}\right|_{a=0} i(t)\,a(x)\sin\omega t+$$
$$+\frac{1}{2}\left.\frac{\partial^2 B}{\partial a^2}\right|_{a=0} i(t)\,a^2(x)\sin^2\omega t+\ldots, \quad (13)$$

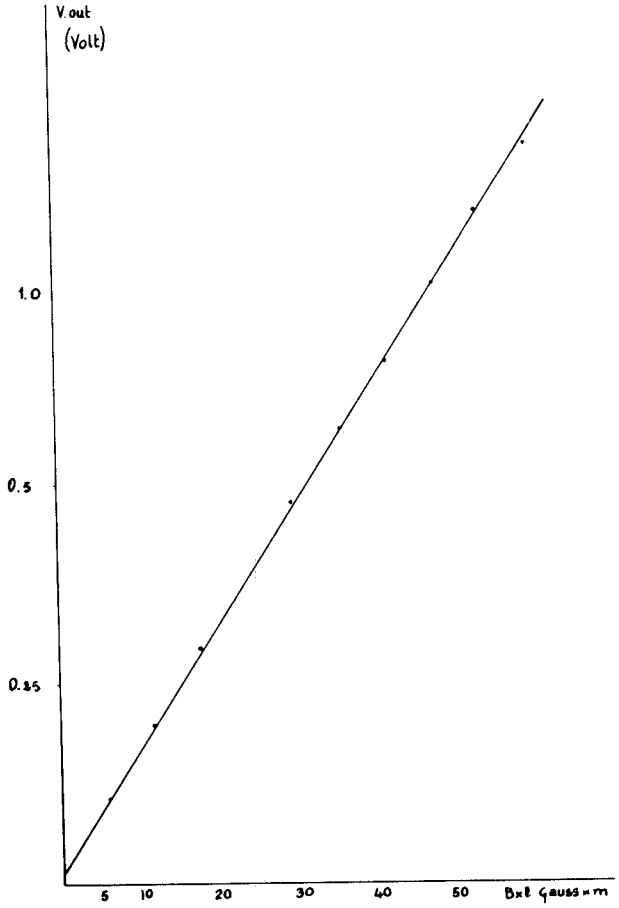

Fig. 7. Magnetometer's output versus bar current.

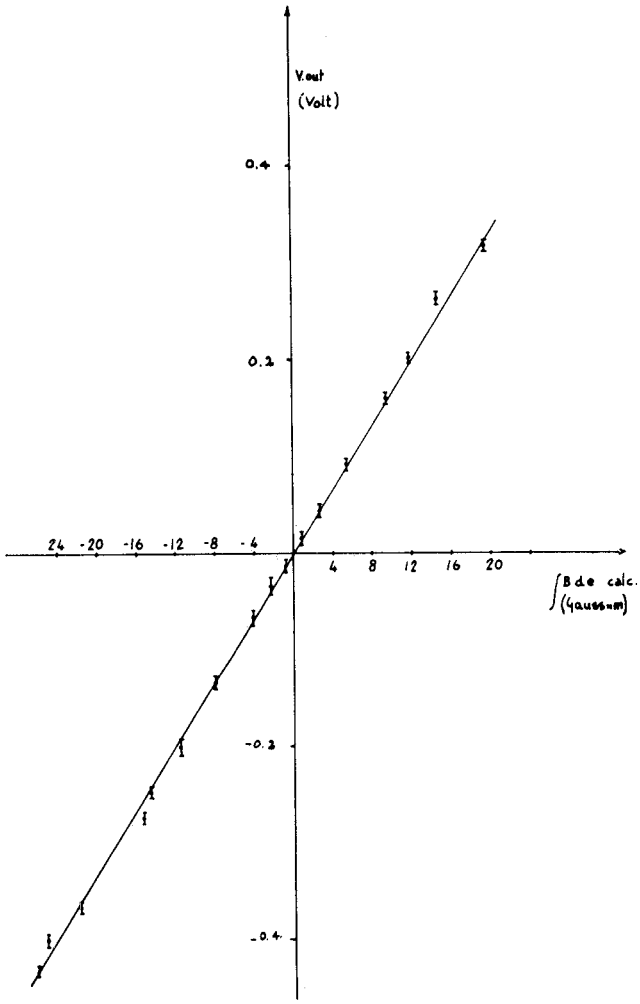

Fig. 8. Magnetometer's output versus sliding contact position.

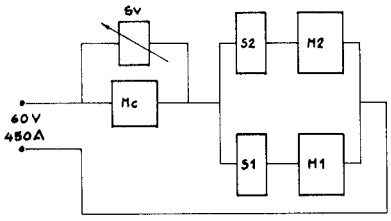

Fig. 9. Scheme of powering the magnets.

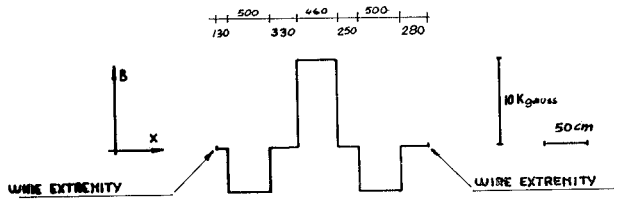

Fig. 10. Field configuration in the row of the magnets.

from which

$$f'(x,t) = \frac{1}{2}\left.\frac{\partial B}{\partial a}\right|_{a=0} i_0\, a^2(x) + \\ + \left[B(x,0) + \left(\left.\frac{\partial^2 B}{\partial a^2}\right|_{a=0} \frac{3a^2(x)}{8}\right)\right] \times \qquad (14)$$
$$\times\, i_0 \sin \omega t - \left.\frac{\partial B}{\partial a}\right|_{a=0} i_0 \frac{a(x)\cos 2\omega t}{2} + \ldots .$$

In our case the results are (see next section):

I. $$\int_0^L \left.\frac{\partial^2 B}{\partial a^2}\right|_{a=0} a^2(x)\,\mathrm{d}x = 0.08\ \mathrm{G\,m};$$

II. $$\int_0^L \left.\frac{\partial B}{\partial a}\right|_{a=0} a(x)\,\mathrm{d}x = 10\ \mathrm{G\,m}.$$

It is therefore necessary (as we see from the size of the term II) to achieve an high rejection of the second harmonic excitation frequency; typically, with the filters we have used, the rejection is about 15:1 and is satisfactory.

4. Experimental tests

In order to obtain the absolute calibration of the magnetometer, we have made measurement in the magnetic field produced by a thin copper bar three meters long parallel to the wire (fig. 6).

The linearity of the system as a function of the current flowing in the bar between M_1 and M_2 is shown in fig. 7.

In fig. 8 we show the behaviour of the signal from the magnetometer as a function of the field integral, which we have calculated from the values of the shunts SH_1 and SH_2.

Obviously there is a position of the contact C corresponding to

$$\int \boldsymbol{B} \times \mathrm{d}\boldsymbol{l} = 0.$$

In this condition also the output signal, after subtraction of coherent background, is zero.

From the graph of fig. 7 it is possible to determine the value of this background (≈ 0.5 G m) which is due essentially to the earth's magnetic field and small stray fields from nearby conductors.

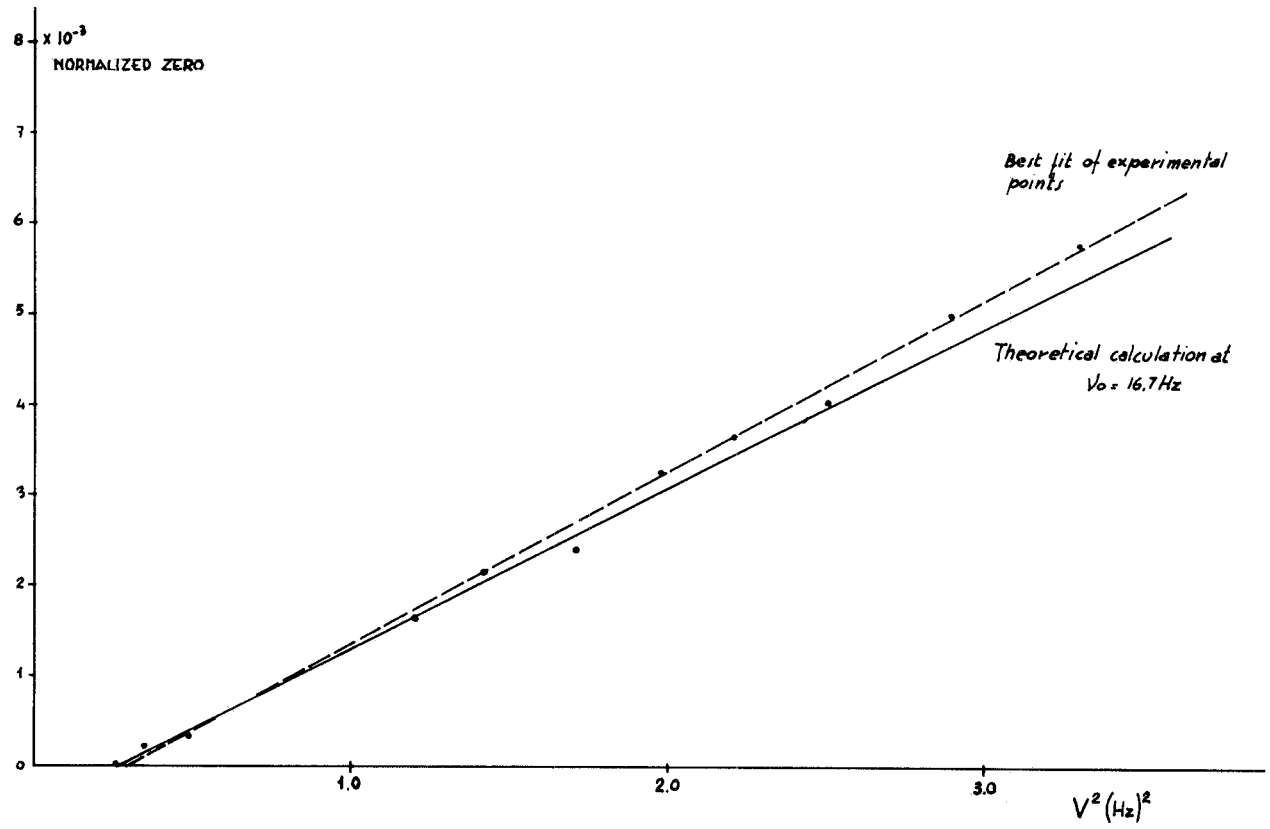

Fig. 11. Normalized zero versus frequency square.

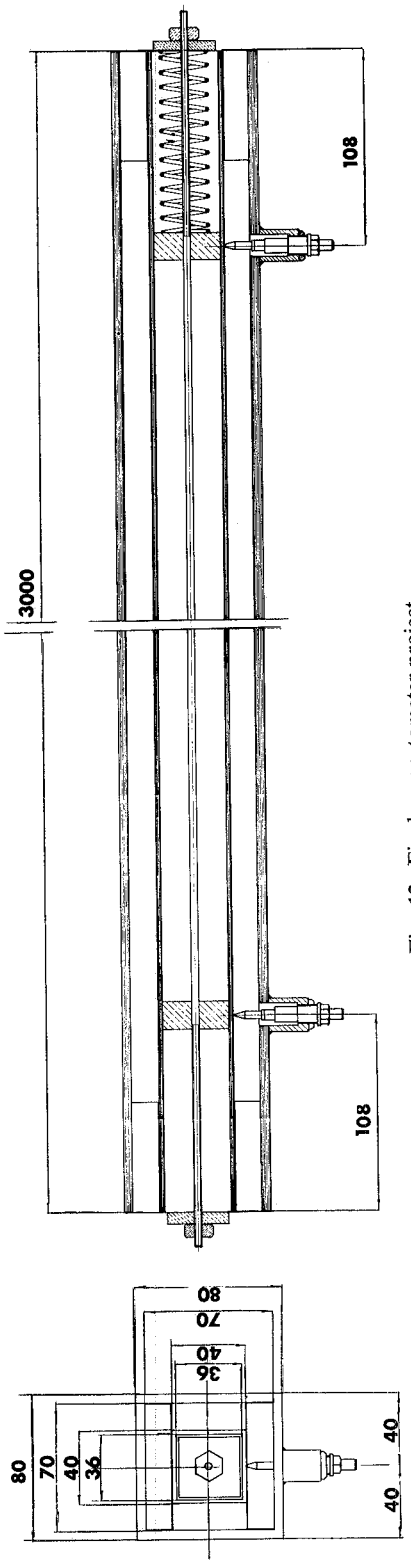

Fig. 12. Final magnetometer project.

We have also carried out measurements using a row of three magnets arranged in such a way to simulate working conditions of the magnetometer. Fig. 9 shows the scheme of powering the magnets while fig. 10 displays the field configuration used.

As can be seen from eq. (5), if the integral of the field is zero the magnetometer output will be zero only in the low frequency limit. This effect and the expected frequency dependence was experimentally tested and is described below.

The field integral is brought to zero by means of the variable shunt SV (see fig. 9) which takes up about 10% of the current of M_c. M_1 and M_2 are magnets with level and parallel poles, while M_e is a magnet having $\partial B/\partial y = 50$ G/cm.

Measurements were carried out as follows: SV was set in order to obtain zero output at drive frequency of 0.5 Hz. Then for each different value of the excitation frequency, we have measured output voltage normalizing by filter response.

The ratio of this voltage to the one obtained when only M_e is on, is plotted against the square of the frequency (fig. 11). The slope of the straight line which fits experimental points is 1.86×10^{-3} Hz^{-2}; this value is to be compared with the calculated value 1.77×10^{-3} Hz^{-2} that we obtain if eq. (5) is applied to each field segment.

Taking into account the approximation we made (step behaviour of magnetic fields, induced currents in the wire, etc.), we can be satisfied with this agreement between theoretical and experimental points. Furthermore we have to consider the effects from the power supply and shunt instabilities; we have tried to minimize these effects with repetition and averaging measurements.

The results we have obtained allow us be confident, that our scheme as described in the previous section, is completely correct.

In particular, we have found that the behaviour of the magnetometer does not depend on the resonance frequency of the wire within 5×10^{-4} (when the magnets are arranged as in fig. 10), if the following condition is fulfilled:

$$v \leqslant v_0/45 .$$

5. Conclusions

The measuring method we have suggested is as sensitive as is required, however our tests on the prototype allow us to plan the following improvements to be carried out when the final magnetometer will be built:

a. the wire will be made of aldry so the first resonating frequency will be about 50 Hz;

b. one of the extremities of the wire will be connected to a spring (see fig. 12) in order to encrease the stability of the mechanical tension;

c. the support will be made more rigid to reduce distortions and allow a higher tension in the wire.

Furthermore we hope to achieve a great improvement in the signal to noise ratio by using a voltage correlator.

It is a pleasure to thank Dr. W. W. Ash for his collaboration.

We are also indebted to Prof. V. Silvestrini and Dr. B. Bartoli for their useful suggestions.

References

[1]) W. W. Ash, D. Grossman, G. Matthiae, G. P. Murtas, M. Nigro, G. K. O'Neill, G. Sacerdoti, R. Santangelo, E. Schiavuta and D. Scannicchio, A magnetic analyzer to be used for Adone colliding beam experiments, Frascati Report LNF-69/2 (1969).

[2]) F. Amman, private communication.